Supplemental material to:

Dislocation-based high-temperature plasticity of polycrystalline perovskite $SrTiO_3$

Lukas Porz[a, b]*, Michael Scherer[a], Marion Höfling[c], Atsutomo Nakamura[d, e], Wolfgang Rheinheimer[f] and Jürgen Rödel[a]

a) Technical University of Darmstadt, Department of Materials and Earth Sciences, Darmstadt, Germany
b) Norwegian University of Science and Technology, Department of Materials Science and Engineering, Trondheim, Norway
c) Technical University of Denmark, Department of Physics, Lyngby, Denmark
d) Osaka University, Department of Mechanical Science and Bioengineering, Osaka, Japan
e) PRESTO, Japan Science and Technology Agency, Saitama, Japan.
f) Forschungszentrum Jülich GmbH, Institute for Energy and Climate Research, Jülich, Germany

*corresponding author: lukas.porz@ntnu.no

Supplemental 1:

A comparison of stress-strain curves was recorded for different grain sizes. The smaller grain size of 1.9±0.3 µm requires much higher stresses for the same total deformation at equal temperature as the larger grain size of 9.3±1.2 µm, as illustrated in Figure S1.

Diffusion-based deformation, e.g., Nabarro-Herring or Coble creep, is typically faster with smaller grain sizes depending on the grain size d with the proportionality of $1/d^2$ and $1/d^3$, respectively. In consequence, a ≈25-fold or ≈125-fold increase in strain rate would be expected for the smaller grain sizes at the same load. Instead, deformation for the smaller grain size requires much higher stresses to achieve the same strain rate. In consequence, diffusion creep can be ruled out.

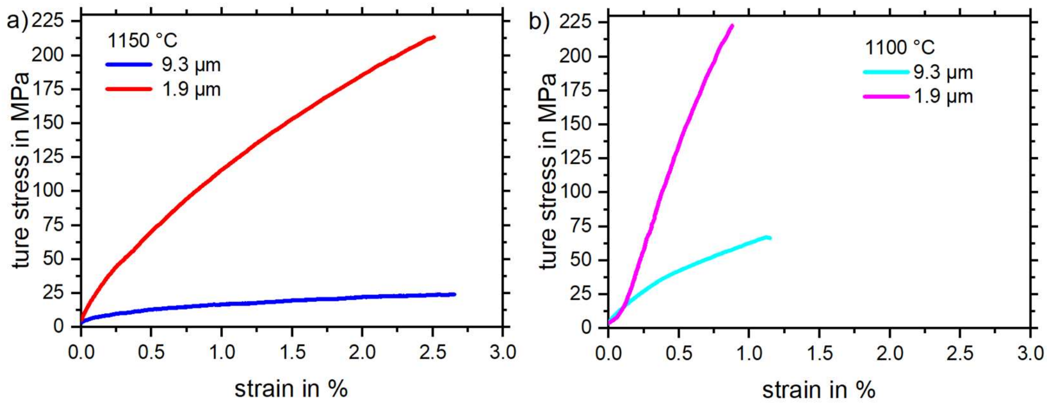

Supplemental Figure 1: Stress strain curves for polycrystalline $SrTiO_3$ for a sample with 9.3±1.2 µm and with 1.9±0.3 µm grain size recorded with a strain rate ($\dot{\epsilon}$) of 10^{-5} s^{-1}. a) 1150 °C. b) 1100 °C.

Supplemental 2:

The effect of deformation history (I) and maximum attainable deformation (II) was checked in a pre-experiment:

(I) First, two strain rate-controlled deformation experiments were done with a strain rate of 10^{-4} s^{-1} (red) to 1 % total deformation each. Despite the intermediate deformation at a strain rate of 10^{-3} s^{-1} (grey), the stress-strain curve featured high reproducibility, indicating deformation independent of the loading history. Second, alternating force-controlled experiments proved reproducibility for a different type of measurement. In contrast to strain rate-controlled experiments, a target force (green and blue) was set and held constant until a significant strain was measured. The strain rate evaluation, which is critical for the construction of the strain rate map, showed no significant differences at 7.5%, 14 %and 18% total strain when the influence of the true stress was considered.

(II) To confirm the integrity of the samples after the severe deformation, the stress was kept constant at 50 MPa until the maximum gauge length of the LVDT was reached (black). Apart from some small chips caused by friction on the base sides with the pistons, the specimen was free of cracks, as shown in the photograph in supplemental Figure 2.

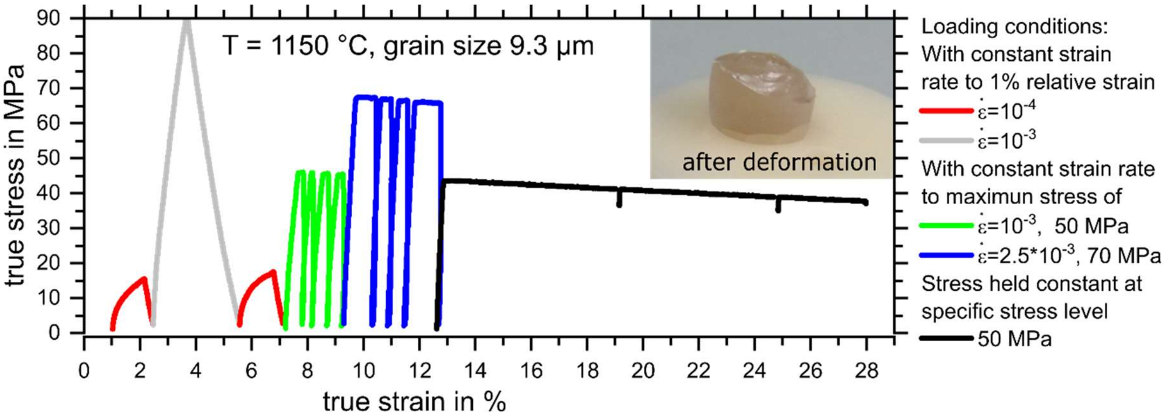

Supplemental Figure 2: Deformation of polycrystalline $SrTiO_3$ under various conditions. First the sample was deformed under strain rate-control marked in grey and red, showing reproducibility among the two red curves with identical parameters. This was followed by several loading steps with different holding times to 50 MPa or 70 MPa, respectively. After this, the stress was held constant at 50 MPa engineering stress until the machine limit was reached. After deformation, the sample was still intact as depicted.

Supplemental 3:

To ascertain reproducibility, two reference samples have been tested. While there appears to be a certain sample-to-sample variation, the trends in the data match as presented in Figure 3:

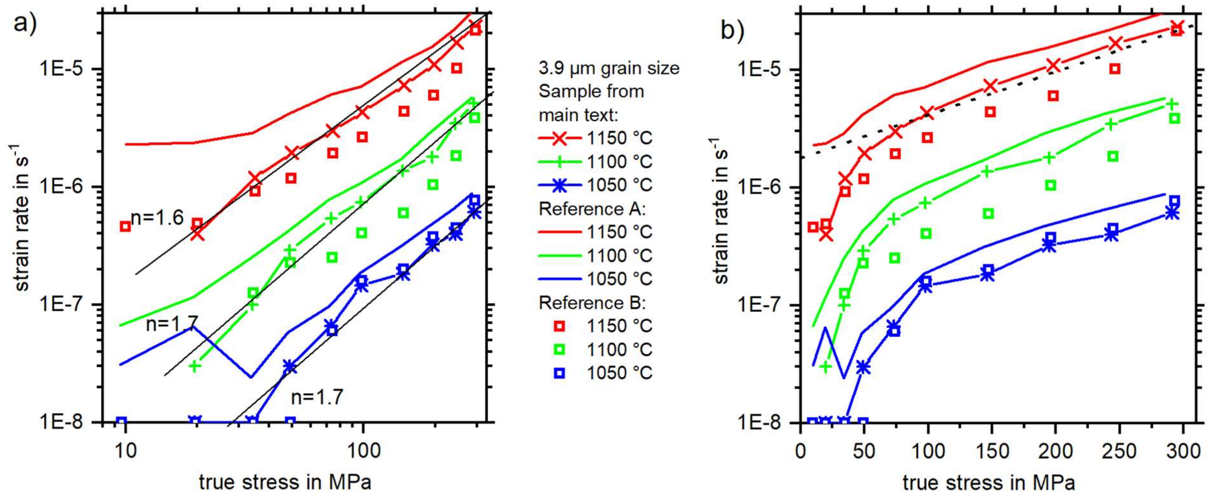

Supplemental Figure 3: Reproducibility check with two reference samples. Data in a) and b) is presented alike to Figure 2 in the main text merely with data points from two additional samples inserted.

Supplemental 4:

Comparison of attainable strain rates in polycrystals to strain rates carried by the <100>{100} and <110>{110} slip system in single crystals. At 1100 °C the strain rate supported by the <110>{110} slip system is about three orders of magnitude lower than the strain rate supported by the <100>{100} slip system. Polycrystals, which need both slip systems to fulfill the Taylor criterion, fall in between. However, the data is noticeably closer to the <110>{110} slip system than the <100>{100} slip system. This points towards a rate-limitation by the <110>{110} slip system in the polycrystal.

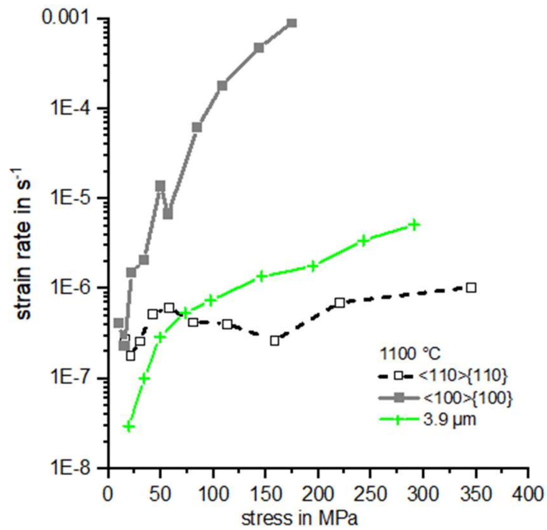

Supplemental Figure 4: Comparison of attainable strain rates at 1100 °C amongst a polycrystals, a single crystal in [110]-loading direction which activates the <100>{100} slip system and a single crystal in [100] load direction which activates the <110>{110} slip system.

Supplemental 5:

In the following TEM image below stemming from a sample of different batch and that has undergone 10.2 % deformation in several steps at 1050 °C to 1150 °C several slip-band like features are visible. The triangular arrangement with one slip plane directly aligned with the line of sight is geometrically not possible to observe with <100>{100} type dislocations. This gives us further confidence, that the <110>{110} slip system needs to be involved in the deformation.

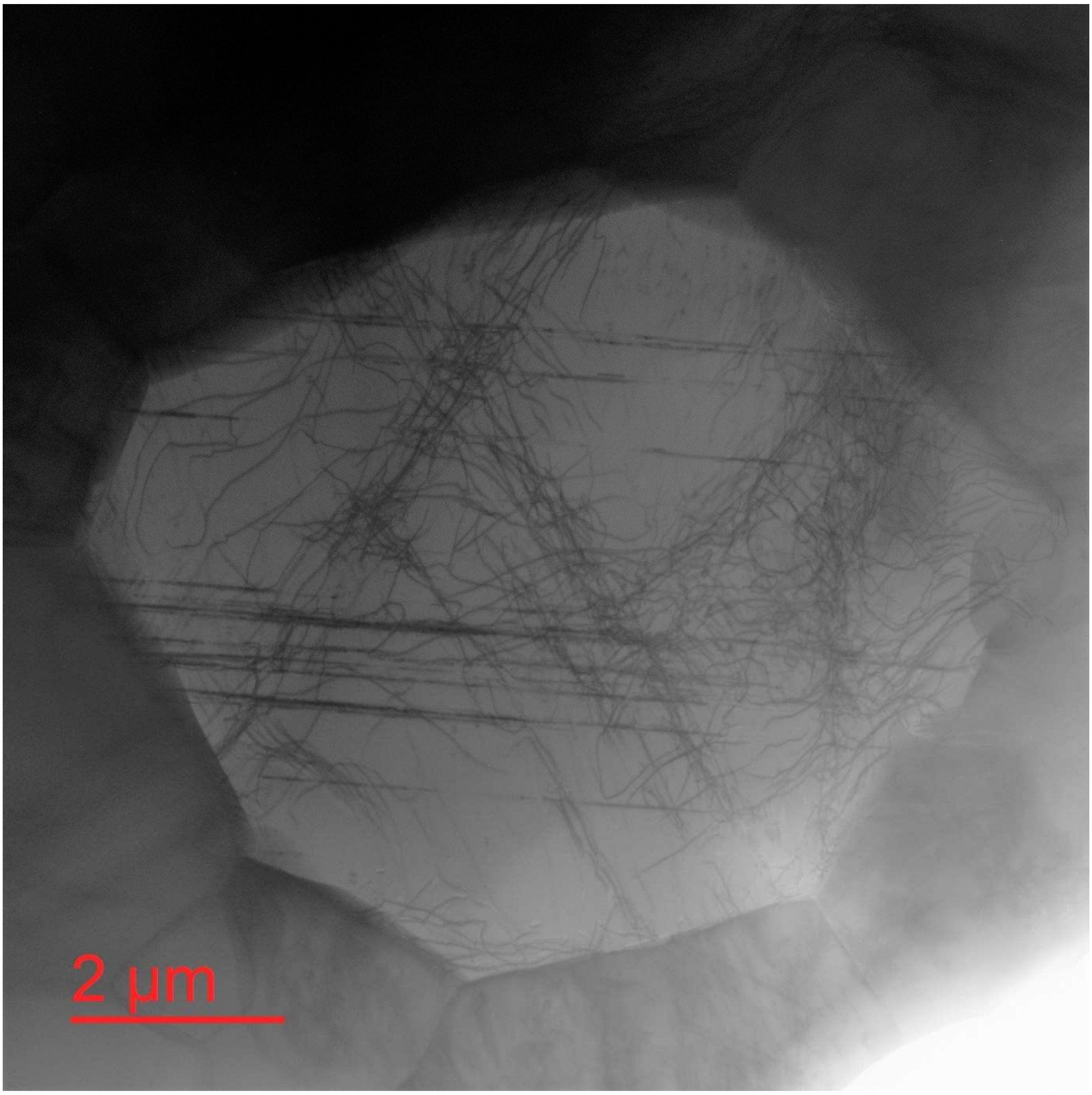

Supplemental Figure 5: Ultra-high voltage electron microscopy image of dislocations in a sample deformed to 10.2 % under varying conditions from the batch with 9.3 µm grain size.